

Structure and mechanical properties of nanocrystalline Ag/MgO composites

TOKUSHI KIZUKA*, HIDEKI ICHINOSE[†], YOICHI ISHIDA[†]*Institute of Industrial Science, University of Tokyo, 7-22-1, Roppongi, Minato-ku, Tokyo 106, Japan*

Nanocrystalline Ag/MgO composites were prepared by the ultrafine-powder-compaction method. The structure was investigated for the first time by high-resolution electron microscopy. Nanometre-sized Ag grains and MgO grains in the composites bonded directly without any intermediate phase layer. Certain preferred orientation relationships were observed between the Ag and MgO grains. The nanocrystalline Ag/MgO composites retained their grain size during annealing up to 873 K. Vickers microhardness measurements were performed on the as-compacted and annealed specimens. Generation and propagation of cracks were less active in the nanocrystalline Ag/MgO composites than in a single-phase nanocrystalline MgO. The Vickers microhardness of the nanocrystalline Ag/MgO composites remained up to 1073 K. Hot-pressing deformation tests showed that the nanocrystalline Ag/MgO composites deformed plastically at 1073 K.

1. Introduction

The mechanical properties of nanocrystalline materials, which are polycrystals with a grain size of the order of a few nanometres differ significantly from those of single crystalline and coarse-grained polycrystalline materials. High ductilities and increases of hardness at ambient temperature have been reported for nanocrystalline ceramics [1] and metals [2, 3], respectively. Superplastic deformation was observed in fine-grained alloys [4] and ceramics [5]. Nanocrystalline materials are expected to deform much more easily than typical superplastic alloys and ceramics. However the structural stability of single-phase nanocrystalline materials at elevated temperature is considerably low [6–7]. In the nanocrystalline metals, the grains begin to grow at just above the ambient temperature [3]. The stability of nanocrystalline materials at elevated temperature has to be improved. It is expected that the two phases composite system with low solubility limits against the constituent elements of the other phase without formation of an intermediate phase, enjoys a good thermal stability.

In the present work, a nanocrystalline composite of a metal and ceramic (Ag/MgO) was prepared by the modified ultrafine-powder-compaction-method. The structure and the thermal stability of the composite were investigated by high-resolution electron microscopy. Vickers microhardness measurements and hot-press deformation tests were also performed.

2. Experimental procedure

MgO fine particles were produced by a gas-condensa-

tion method [8]: Mg (99.99 at %) was evaporated from a tungsten heater after an ultrahigh vacuum chamber was evacuated to 10^{-6} Pa and a gaseous mixture of 80% helium and 20% oxygen at a pressure of 10^4 Pa was introduced. MgO fine particles moving upward with the gas flow were collected on the surface of a rotating stainless cylinder, which was cooled to nitrogen temperature. Subsequently, ultrafine particles of Ag were produced by an inert-gas evaporation method [9]: Ag (99.999 at %) was evaporated on a tungsten heater after restoring the vacuum chamber to 10^{-6} Pa and helium with a pressure of 10^2 Pa was introduced. Ag ultrafine particles moving upward adhered to the surface of MgO fine particles on the cylinder. After restoring the vacuum chamber to 10^{-6} Pa, MgO and Ag ultrafine particles were scraped off the cylinder and compacted under an applied pressure of 2×10^9 Pa into a disk 5 mm in diameter and 0.4 mm thick. The nanometre-sized particles were not exposed to air before compaction.

Isochronal annealing was carried out at temperatures ranging from 293 K to 1073 K in 1.8×10^3 s in a vacuum of 10^{-4} Pa.

X-ray diffraction (XRD) measurements were performed on as-compacted and annealed specimens.

Disk-shaped specimens were cut into a wedge shape by a razor blade and then polished by Ar^+ -ions accelerated to 3 kV. The polished specimens were observed by high-resolution electron microscopy (JEM-200CX and JEM-4000EX).

As-compacted and annealed specimens were indented by a Vickers diamond pyramid over a peak-load range of 1–2 N with a dwell time of 20 s.

* Authors' present addresses: Department of Applied Physics, School of Engineering, Nagoya University, Furo-cho, Chikusa-ku, Nagoya, 464, Japan. [†] Department of Materials, Faculty of Engineering, University of Tokyo, 7-3-1, Hongo, Bunkyo-ku, Tokyo, 113, Japan.

Hot-press deformation tests were performed at 673, 873 and 1073 K, with an applied pressure of 10^8 Pa.

3. Results and discussion

3.1. Structure

Fig. 1 shows the bright-field image of the Ag and MgO ultrafine particles collected on the cylinder. Single crystalline and multiple twinned Ag particles adhere directly to cubic-shaped MgO particles whose surfaces are parallel to the $\{100\}$ planes. The composite particles are mixed homogeneously before the compaction.

Fig. 2a and b show the bright-field image and selected-area diffraction pattern of an as-compacted

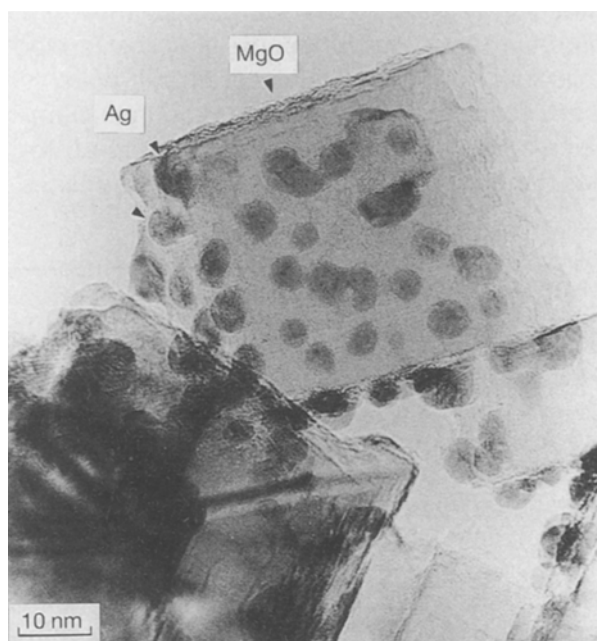


Figure 1 A bright-field image of Ag and MgO ultrafine particles before compaction.

specimen, respectively. The ring pattern in Fig. 2b shows that no preferred orientation exists macroscopically in the as-compacted specimen. All the diffraction rings were attributed to Ag and MgO; no intermediate reaction phase was identified. XRD tests also showed the same result. The mixing ratio of Ag and MgO was estimated to be about 24 mass % Ag according to the reflection intensity ratio of 111_{Ag} and 200_{MgO} of the XRD. Fig. 3 shows a high-resolution image of as-compacted specimen. In Fig. 3 lines without a letter *M* indicate $\{111\}$ lattice fringes of Ag, while lines with a letter *M* indicate $\{200\}$ lattice fringes of MgO. Small arrows indicate $\{111\}$ $\Sigma = 3$ twin boundaries of Ag. The average size of the Ag and MgO grains was 2–20 nm and 2–50 nm, respectively, as shown in Fig. 2a and in Fig. 3. Some of the Ag grains which aggregated around the large MgO grains had a preferred orientation; that is

$$(a) (\bar{1}11) [110]_{\text{Ag}} \parallel (001) [010]_{\text{MgO}}$$

as denoted by bold arrows in Fig. 3. The atomic arrangement of the Ag/MgO interface in the orientation relationship (a) is shown schematically in Fig. 4a. However, the other Ag grains did not align in the preferred orientation.

Three kinds of nanometre-sized boundaries, (that is, Ag/Ag, MgO/MgO grain boundaries and Ag/MgO interphase boundary) exist in the nanocrystalline Ag/MgO composite. Most of the Ag/Ag and MgO/MgO grain boundaries except $\{111\}$ $\Sigma = 3$ twin were general boundaries. The characteristics of the Ag/Ag and MgO/MgO grain boundaries are similar to those in single-phase nanocrystalline Ag [3] and nanocrystalline MgO [10], indicating the slightness of the influence of the composite formation on the nature of these grain boundaries in as-compacted specimens.

Fig. 5 shows a high-resolution image of isolated Ag grains 2 nm in size on MgO grains in an as-compacted specimen. The isolated single crystalline Ag grains had

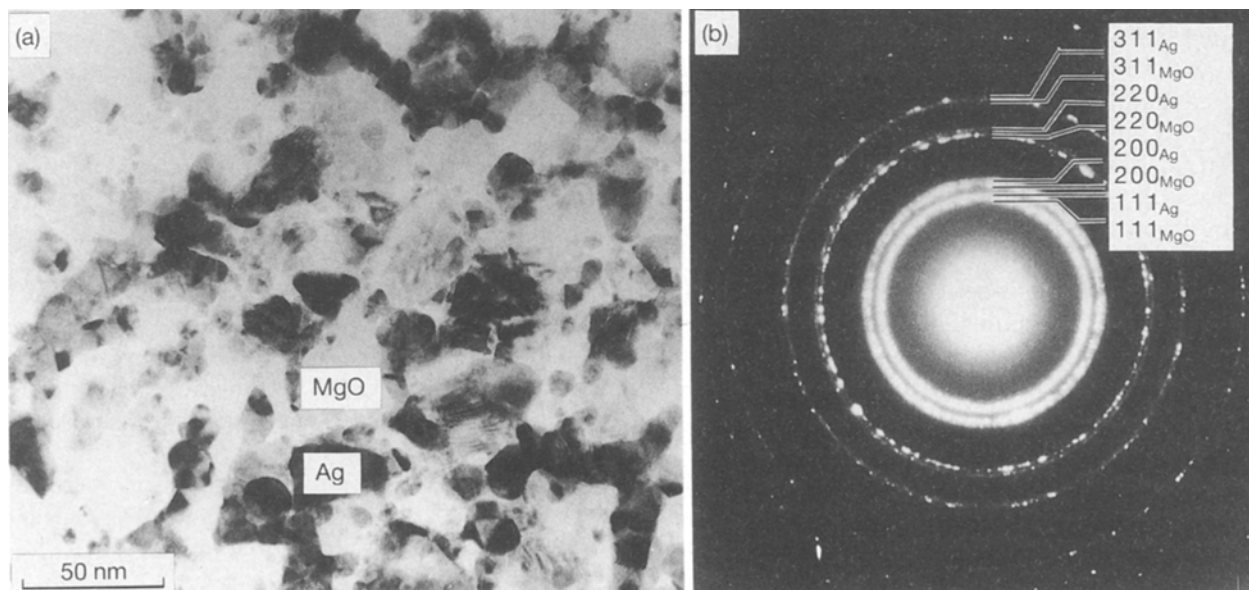


Figure 2 (a) The bright-field image of an as-compacted nanocrystalline Ag/MgO composite and (b) the selected-area diffraction pattern.

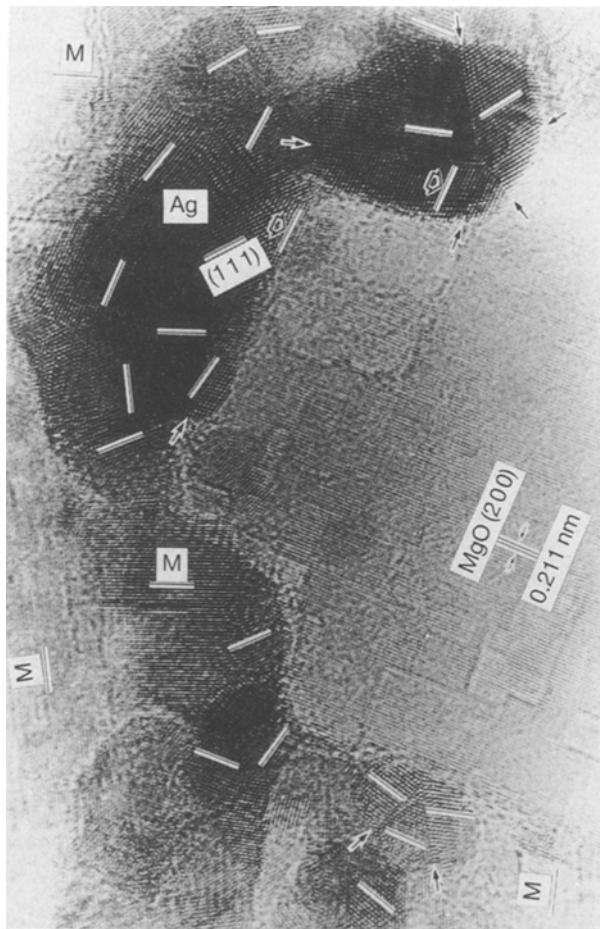


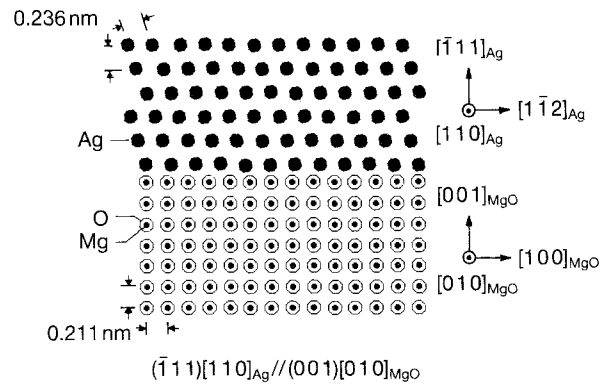
Figure 3 A high-resolution image of an as-compacted nanocrystalline composite. The small arrows indicate $\{111\} \Sigma = 3$ twin boundaries of Ag. The bold arrows are described in text.

a tendency to align with MgO grains in a particular orientation; that is

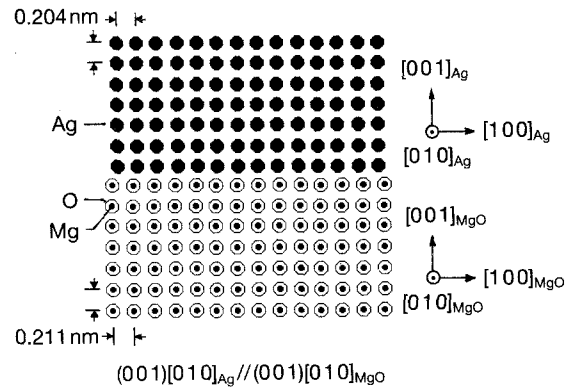
$$(b) (001) [010]_{Ag} \parallel (001) [010]_{MgO}$$

as shown in Fig. 5. The orientation relationship (b) is shown schematically in Fig. 4b. In this special orientation relationship, the lattice misfit at the interface is small, being approximately 3%. In fact, in vacuum-deposition, Ag crystals with a grain size of a few tens of nanometres were found to grow epitaxially on an air-cleaved MgO (100) surface without heat treatment according to Harada *et al.* [11]. The nanometre-sized Ag/MgO interface at which the orientation relationship (a) or (b) was satisfied, are inferred to be stable in the composite. The present high-resolution observation, however, showed that not all the Ag grains aggregated around the large MgO grain aligned in the two preferred orientations, as shown in Fig. 3.

Single-crystalline Ag particles, and multiple twinned Ag particles, which were the aggregation of some Ag crystallites containing the $\{111\} \Sigma = 3$ twin boundaries [12], were produced by the inert-gas-evaporation method [13]. Single-crystalline Ag particles can rotate to a stable orientation, such as (a) and (b) on the MgO grains. When the multiple twinned Ag particles adhere to the MgO grains, only one of the Ag grains can orient in the relationship (a) or (b). It is



(a)



(b)

Figure 4 Schematic diagrams of the atomic arrangement of the Ag/MgO interfaces in the two preferred orientation relationships. The relationship (a) is observed in the Ag grains aggregated surrounding the larger MgO grains. The relationship (b) is observed in the isolated Ag grains on the MgO grains.

deduced that most of the Ag grains did not orient in the relationship (a) or (b) for this reason; the Ag/Ag grain boundaries prevent the rotation of the Ag grains on the MgO grains.

In addition to the orientation, the five kinds of bonding, (that is, Ag–Ag, Mg–Mg, O–O, Ag–O and Ag–Mg) should be taken into account in order to evaluate the boundary structure. It is suggested that various types of atomic arrangement exist in the boundaries in the nanocrystalline Ag/MgO composites.

3.2. Thermal stability

Fig. 6a and b show bright-field images of specimens annealed at 873 and 1073 K, respectively. X-ray and selected-area diffraction analysis showed no formation of an intermediate reaction phase in the specimens annealed at these temperatures. No change of grain shape and grain size was observed in the specimen annealed at 873 K, as shown in Fig. 6a. The Ag grains grew to 10–30 nm in size and contained $\{111\} \Sigma = 3$ twin boundaries, and MgO grains with sizes less than 25 nm also grew to 25–50 nm in the specimen annealed at 1073 K, as shown in Fig. 6b. The shape of the MgO grains changed from cubic to an undefined shape. Grain growth in single-phase nanocrystalline MgO also started at 1073 K [10]. Grain growth in

single-phase nanocrystalline Ag started at 373 K and the grain size was 80–300 nm at 673 K, 300–500 nm at 873 K and 300–1000 nm at 1073 K [3]. No growth of Ag grains was observed even at 873 K in the present Ag/MgO interphase boundaries and the MgO/MgO grain boundaries prevent the growth of Ag grains.

3.3. Indentation fracture morphology and Vickers microhardness

Fig. 7a and b show optical micrographs of the surface of 1 N and 2 N indentations, respectively, in single-

phase nanocrystalline MgO and Fig. 7c shows an as-compacted nanocrystalline Ag/MgO composite. No crack was observed in nanocrystalline MgO after the 1 N indentation as shown in Fig. 7a. The contact impression and associated cracks emanating from it

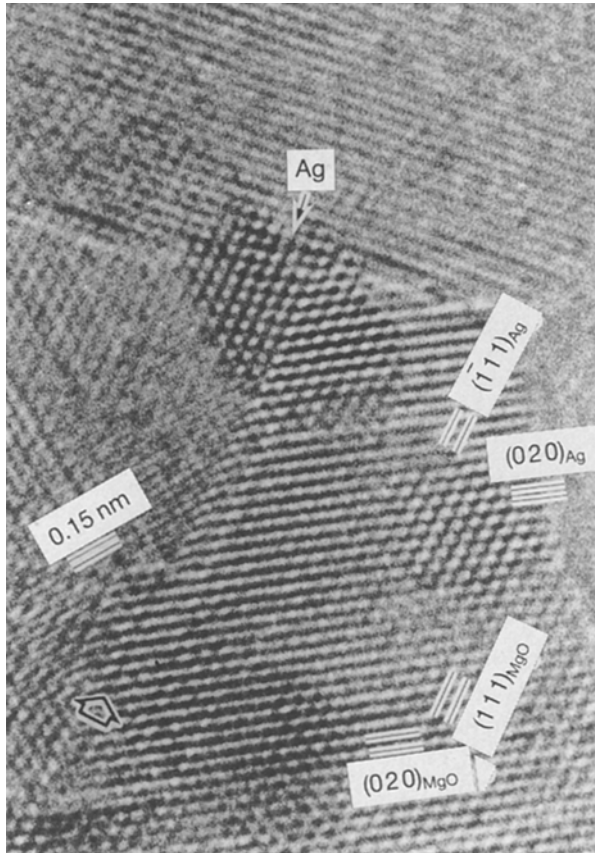


Figure 5 A high-resolution image of isolated Ag grains on MgO grains in an as-compacted nanocrystalline Ag/MgO composite. The bold arrow indicates the $\{111\} \Sigma = 3$ twin boundary of MgO.

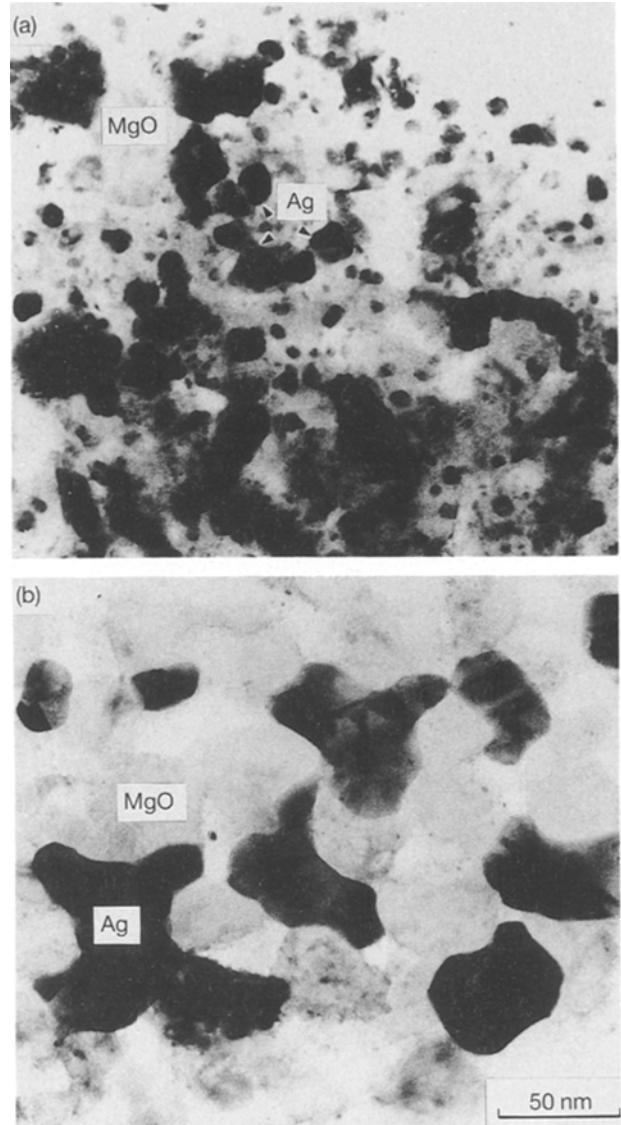


Figure 6 Bright-field images of the specimen annealed at: (a) 873 K, and (b) 1073 K.

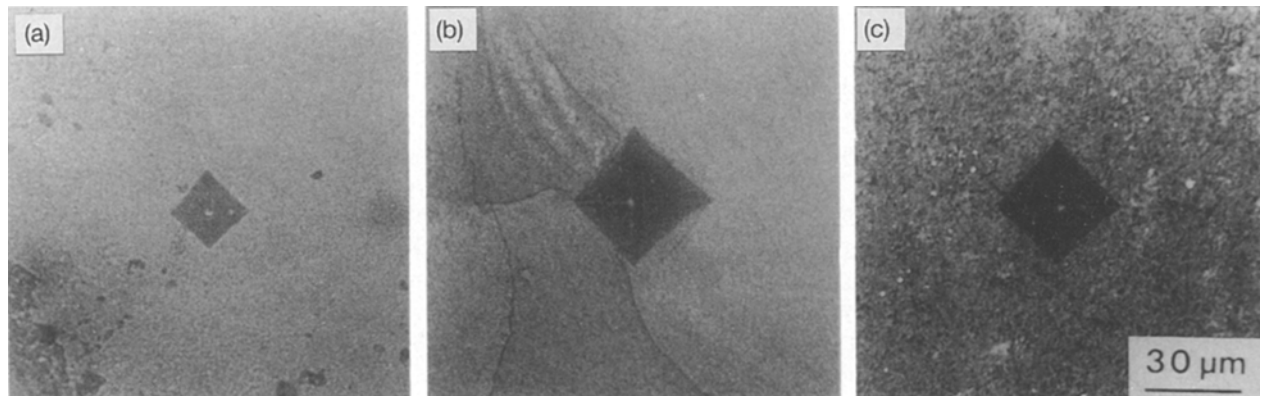


Figure 7 Optical micrographs after indentation by a Vickers diamond pyramid on the surface of: (a) and (b) single-phase nanocrystalline MgO, and (c) nanocrystalline Ag/MgO composite. The pressure applied was 1 N in (a) and 2 N in (b) and (c); the dwell time was 20 s.

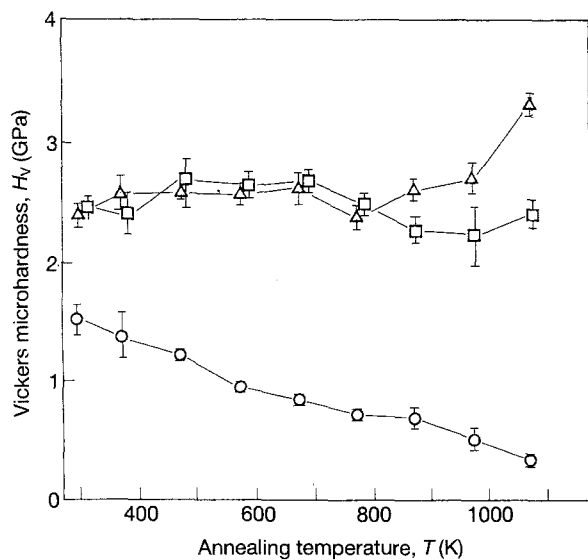


Figure 8 (□) The variation of the Vickers microhardness for a nanocrystalline Ag/MgO composite with an applied pressure of 1 N after isochronal annealing. For comparison, the Vickers microhardness of (○) a single-phase nanocrystalline Ag and (△) nanocrystalline MgO are also shown.

were observed in nanocrystalline MgO after the 2 N indentation as shown in Fig. 7b. On the other hand, no crack was observed in the nanocrystalline Ag/MgO composite for the 2 N indentation as shown in Fig. 7c. It was found that the addition of nanometre-sized Ag crystallites to nanocrystalline MgO prohibits the generation and propagation of cracks.

Fig. 8 shows variation of the Vickers microhardness measured in a nanocrystalline Ag/MgO composite under an applied pressure of 1 N after isochronal annealing. For comparison, the Vickers microhardness of nanocrystalline Ag and nanocrystalline MgO are also shown in Fig. 8. The Vickers microhardness of nanocrystalline MgO does not change in the temperature range from 293–973 K but it increases in the range 973–1073 K. This increase of the hardness results from neck growth which proceeds above 973 K in nanocrystalline MgO, as reported by Kizuka [10]. The microhardness of nanocrystalline Ag decreased monotonically from 293 to 1073 K as the grain size increased, suggesting that the decrease of the microhardness can be attributed to grain coarsening [3]. The microhardness of the nanocrystalline Ag/MgO

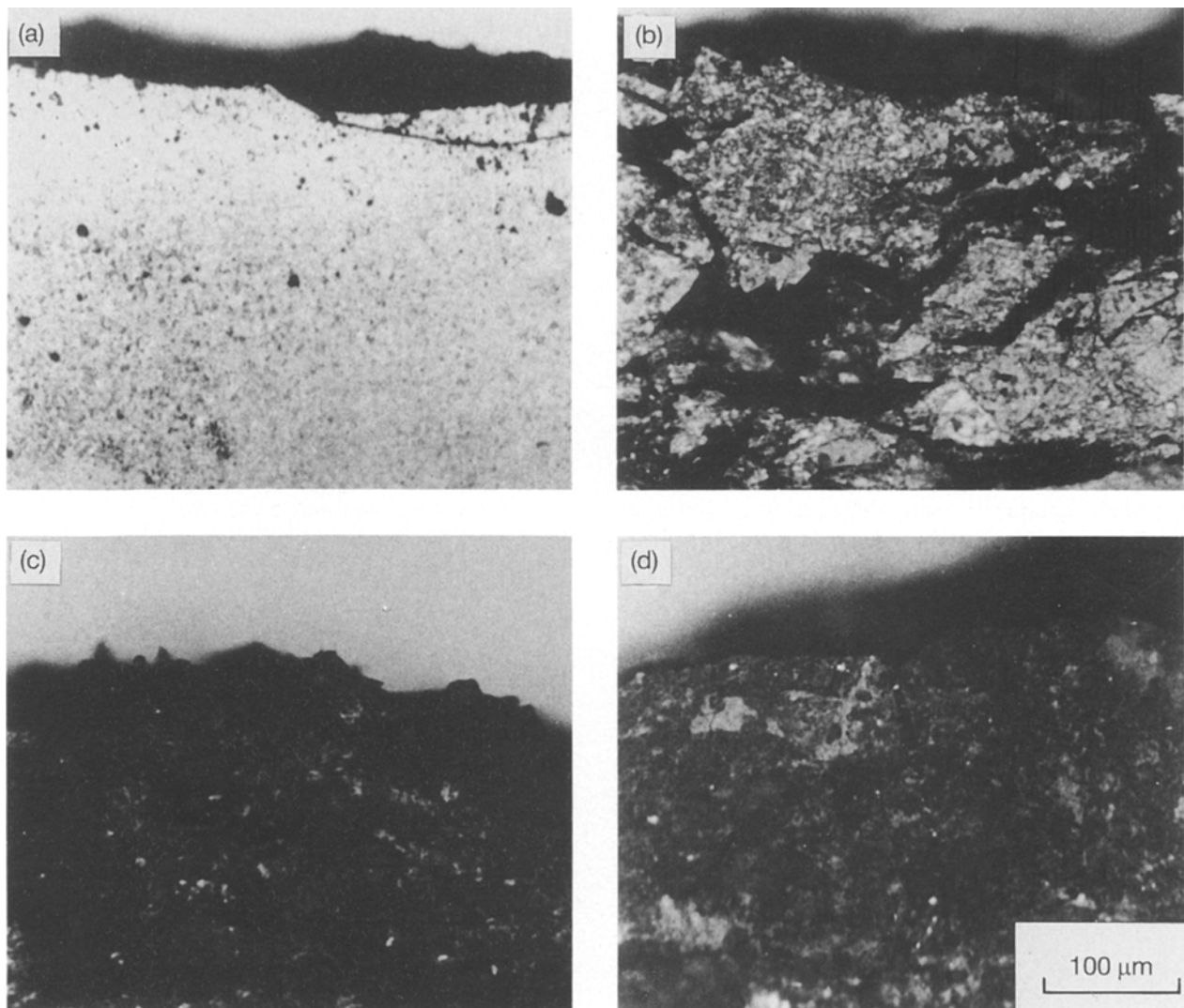


Figure 9 Optical micrographs of the surface near the edge of (a) an as-compacted nanocrystalline Ag/MgO composite, and of specimens pressed with an applied pressure of 100 MPa at: (b) 673 K, (c) 873 K, and (d) 1073 K.

composite is similar to that of the nanocrystalline MgO in the temperature range 293–873 K. The microhardness of the nanocrystalline Ag/MgO composite did not change during annealing in the temperature range 873–1073 K in spite of the grain coarsening. The Vickers microhardness of the present specimen was unchanged after annealing even at 1073 K.

3.4. Hot-press deformation

Fig. 9a to d shows optical micrographs of the surface near the edge of an as-compacted nanocrystalline Ag/MgO composite and specimens pressed with an applied pressure of 10^8 Pa at 673, 873 and 1073 K, respectively. The thickness reductions p ($= d_f/d_i$, d_i and d_f are the thicknesses of the pellet before and after the hot-pressing), at 673, 873 and 1073 K are 81%, 64% and 65%, respectively. A number of cracks propagated in undefined directions in the specimens pressed at 673 and 873 K. The value of the thickness reduction of the specimen pressed at 1073 K is similar to that of the specimen pressed at 873 K. However, the number of radial cracks generated from the centre decreased significantly. The decrease indicated the presence of plastic deformation in the nanocrystalline Ag/MgO composite at 1073 K. No structural change was observed by high-resolution electron microscopy between the specimen pressed at 1073 K and the specimen annealed at same temperature; this suggests that the boundary sliding contributed to the plastic deformation of the nanocrystalline Ag/MgO composite at 1073 K.

4. Conclusions

Nanocrystalline Ag/MgO composites were prepared by the ultrafine-powder-compaction method. Their structure was investigated for the first time by high-resolution electron microscopy. The Vickers microhardnesses were measured for the as-compacted and annealed specimens. Hot-press deformation tests were also performed on them. It is found that the structure and mechanical properties of the nanocrystalline Ag/MgO composite were different from those of single-phase nanocrystalline Ag or MgO in the following points.

1. Nanometre-sized Ag grains and MgO grains in as-compacted and annealed specimens bonded directly without any intermediate phase layer. The two preferred orientation relationships, that is,

$$(a) (\bar{1}11) [110]_{\text{Ag}} \parallel (001) [010]_{\text{MgO}}$$

$$(b) (001) [010]_{\text{Ag}} \parallel (001) [010]_{\text{MgO}}$$

were observed between Ag and MgO grains.

2. The nanocrystalline structure of the present specimen was stable up to 873 K. The Vickers microhardness did not change during annealing at 1073 K.

3. The generation and propagation of cracks in the as-compacted nanocrystalline Ag/MgO composite was less enhanced than in single-phase nanocrystalline MgO.

4. The nanocrystalline Ag/MgO composite deformed plastically at 1073 K.

Acknowledgements

The authors thank Professor Kouji Hayashi of Institute of Industrial Science, University of Tokyo for assistance with Vickers microhardness measurements, and Dr Manuel E. Brito of the National Institute for Research in Inorganic Materials and Dr K. Ibe of JEOL for help with the use of the high-resolution electron microscopes. We also wish to thank the Miyashita Research Foundation for Materials Science, The Kazato Foundation and the Murata Science Foundation for generous financial assistance. This study was partly supported by a Grant-In-Aid of the Ministry of Education in the Priority-Area Research.

References

1. J. KARCH, R. BIRNINGER and H. GLEITER, *Nature* **330** (1989) 556.
2. G. W. NIEMAN, J. R. WEERTMAN and R. W. SIEGEL, *Scripta Metall.* **23** (1989) 2013.
3. T. KIZUKA, H. ICHINOSE and Y. ISHIDA, *Philos. Mag. A* **69** (1993) 551.
4. J. W. EDINGTON, K. N. MELTON and C. P. CUTLER, *Prog. Mater. Sci.* **21** (1976) 61.
5. F. WAKAI, S. SAKAGUCHI and Y. MATSUNO, *Adv. Ceram. Mater.* **1** (1986) 259.
6. H. E. SCHAEFER, R. WÜRCHUM, R. BIRNINGER and H. GLEITER, *Phys. Rev. B* **38** (1988) 9545.
7. R. W. SIEGEL, S. RAMASWAMY, H. HAHN, LI ZONGQUAN, LU TING and R. GRONSKY, *J. Mater. Res.* **3** (1988) 1367.
8. C. KAITO, K. FUJITA and J. SHIOJIRI, *J. Appl. Phys.* **47** (1967) 5161.
9. K. KIMOTO, Y. KAMIYA, M. NONOYAMA and R. UYEDA, *Jpn. J. Appl. Phys.* **2** (1963) 702.
10. T. KIZUKA, Doctoral thesis, University of Tokyo, (1991).
11. T. HARADA, M. ASANO and Y. MIZUTANI, *J. Cryst. Growth* **116** (1992) 243.
12. K. MIHAMA and Y. YASUDA, *J. Phys. Soc. Jpn.* **21** (1966) 1166.
13. K. KIMOTO and I. NISHIDA, *J. Phys. Soc. Jpn.* **22** (1967) 940.

Received 16 September
and accepted 17 December 1993